

## Supporting Informations

### Enhanced visible-light-induced photocatalytic activities of bimetallic Mn-Fe MOFs for highly efficient reductive removal of Cr(VI)

Zohreh Garazhian, Alireza Farrokhi\*, Abdolreza Rezaeifard\*, Maasoumeh Jafarpour and Rouhollah khani

Department of Chemistry, Faculty of Science, University of Birjand, Birjand, 97179-414 Iran.

#### Preparation of bimetallic MOFs

**STA-12(Mn, Fe) [(0.5Mn + 0.5Fe)<sub>2</sub>L.4.14H<sub>2</sub>O]**: Ferrous chloride tetrahydrate (Merck, 0.256 g, 1.29 mmol), Manganese(II) acetate tetrahydrate (Merck, 0.316 g, 1.29 mmol), H<sub>4</sub>L (0.355 g, 1.29 mmol), potassium hydroxide (Merck, 0.218 g, 3.9 mmol) and water (20 mL) were mixed, to give a reaction ratio of 1:1:1:3:900, in a Teflon lined autoclave (40 mL). The reaction was stirred for 1h and an initial pH of 5.5 was recorded. The autoclave was then sealed and heated at 180 °C for 72 h. The resulting powder was collected by filtration, washed with water, and dried overnight at 50 °C. The other MOFs were obtained by change of percentages of Fe:Mn while the other conditions were invariable. Elemental mapping of Mn and Fe using energy dispersive spectroscopy (EDS) are depicted in Figure S8, indicating that these elements are homogeneously distributed and co-localized throughout the MOFs. (for more information on catalysts identification and data analysis, see Table S1 and Figure S5-S9 and reference<sup>19</sup>).

**Table S1.** ICP (ICP-AES) Elemental analysis results for as-prepared MOFs.

STA-12-Mn-Fe	Mn%	Fe%
(80:20)	15.18	8.46
(70:30)	14.27	9.51
(50:50)	11.80	11.86
(30:70)	9.41	14.33
(20:80)	8.38	15.47

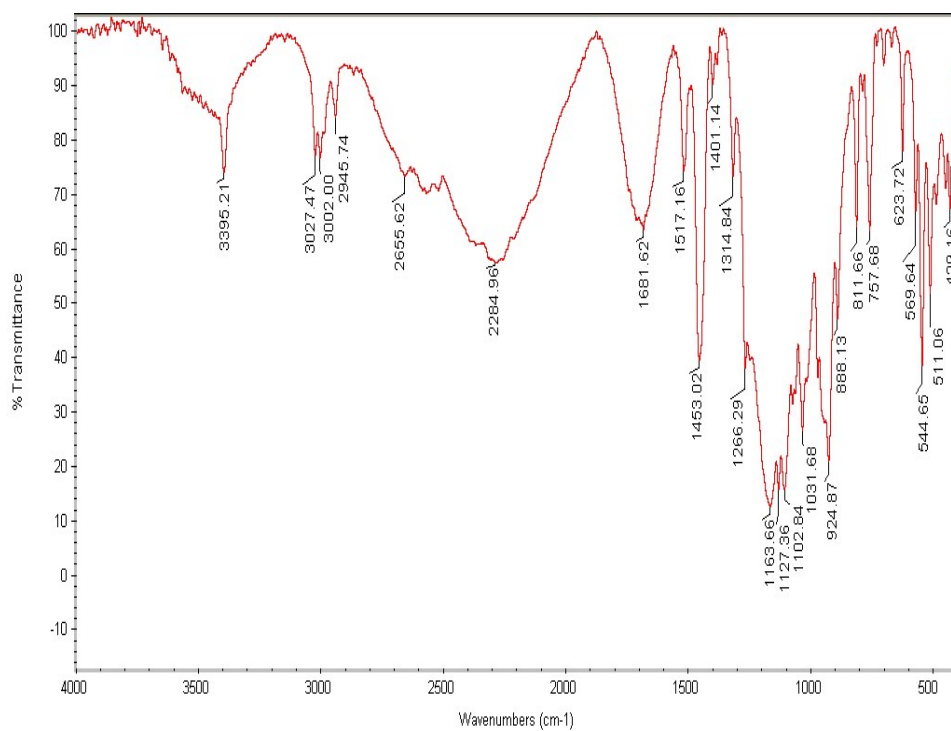


**Fig. S1.** IR spectrum of Ligand H<sub>4</sub>L.

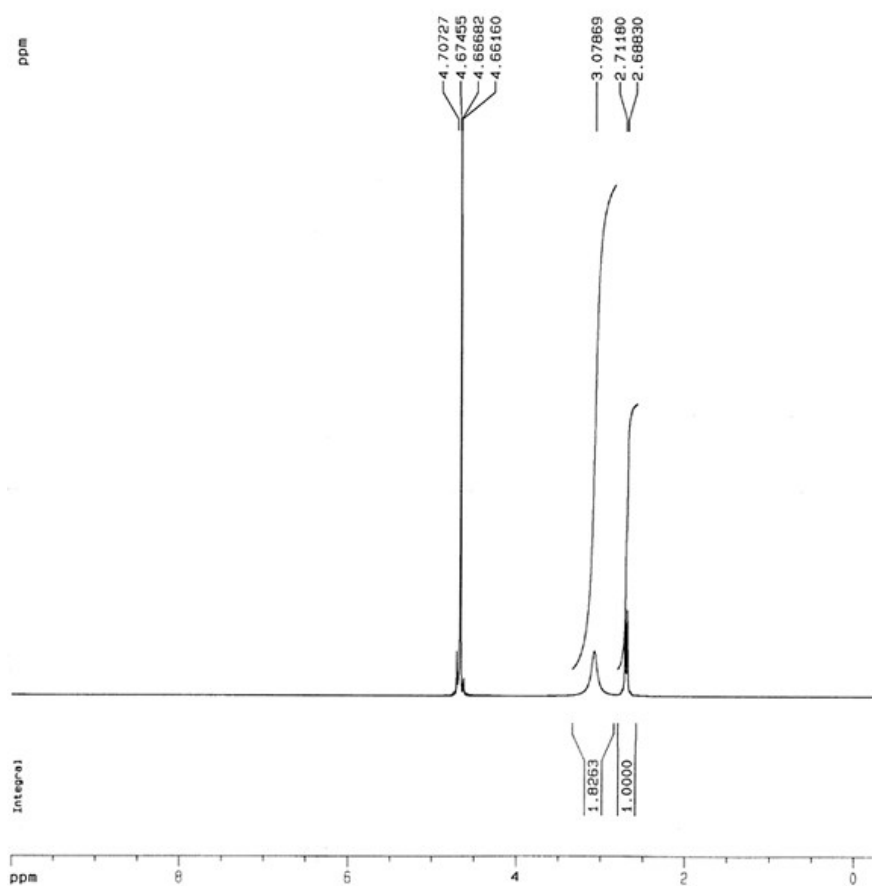


**Fig. S2.** <sup>1</sup>H NMR spectrum of Ligand H<sub>4</sub>L.

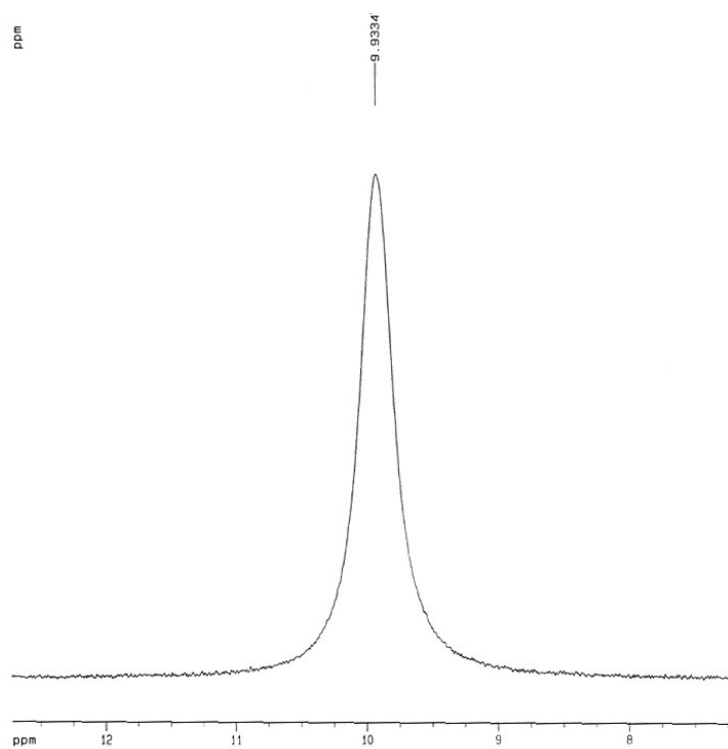


**Fig. S3.**  $^{31}\text{P}\{\text{H}\}$  NMR spectrum of Ligand  $\text{H}_4\text{L}$ .

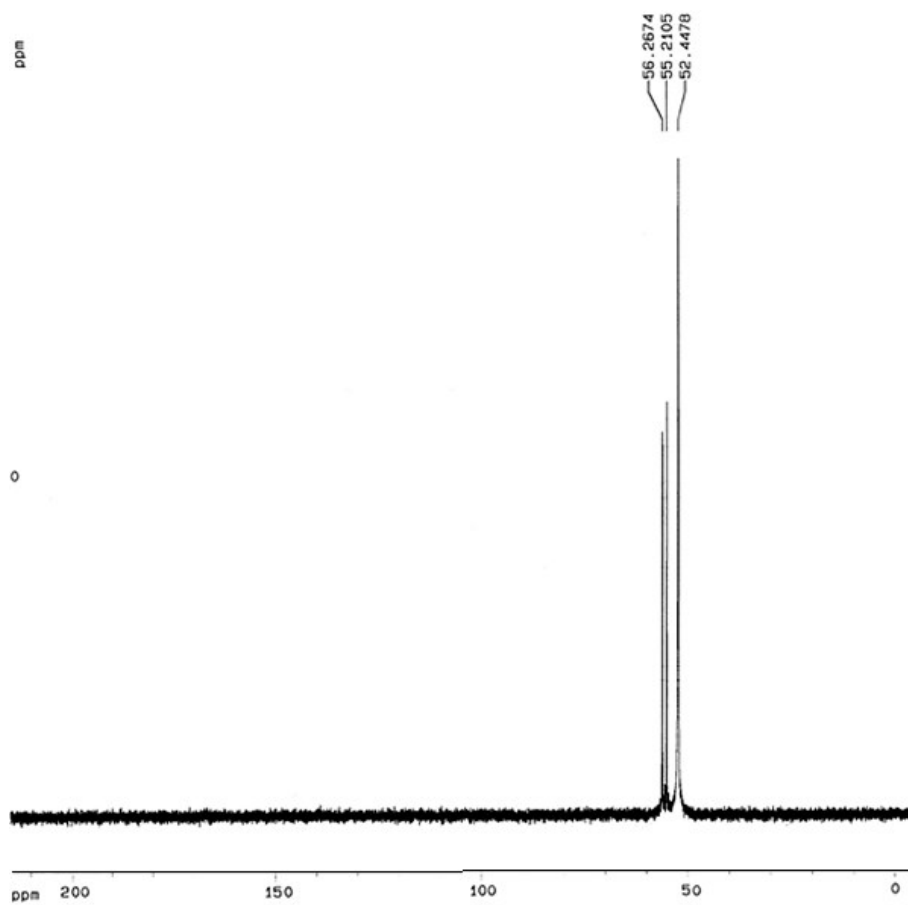


**Fig. S4.**  $^{13}\text{C}$  NMR spectrum of Ligand  $\text{H}_4\text{L}$ .

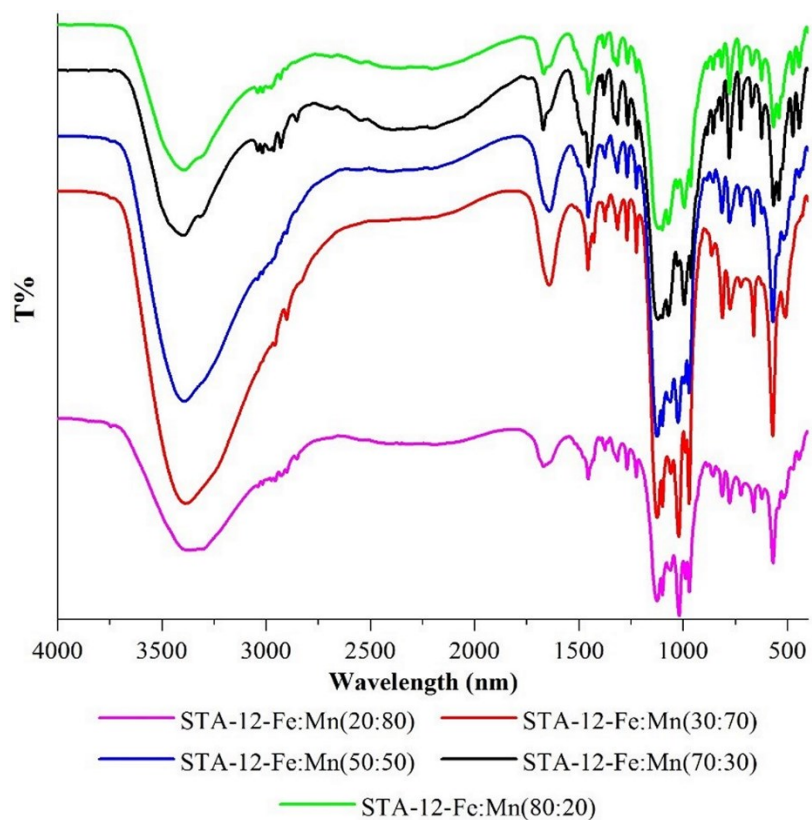


**Fig. S5.** FT-IR spectra of STA-12-Mn-Fe MOFs.

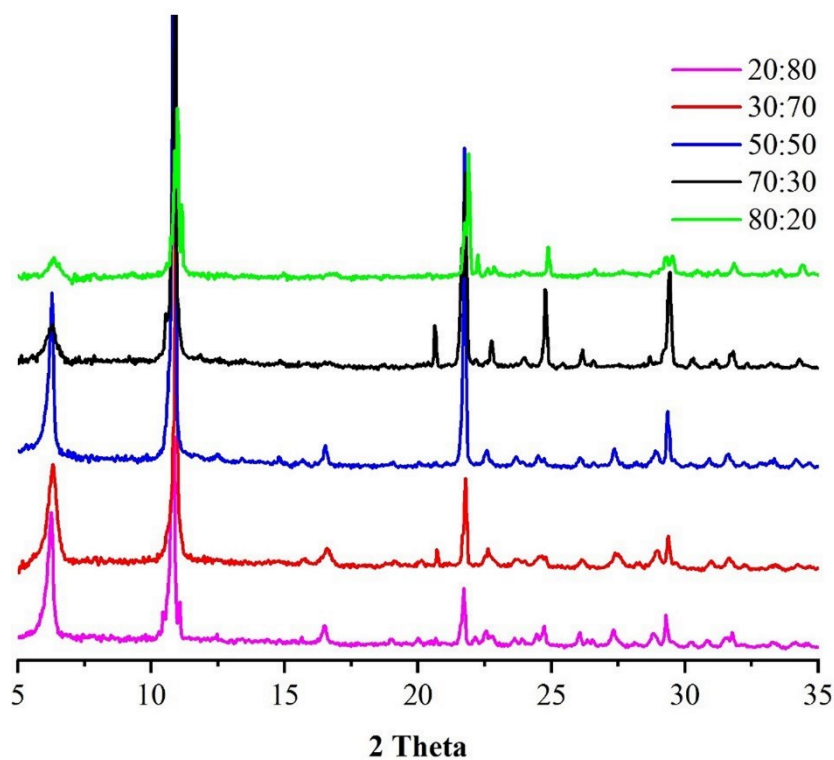


**Fig. S6.** X-ray diffraction patterns of STA-12-Mn-Fe MOFs.<sup>[1]</sup>

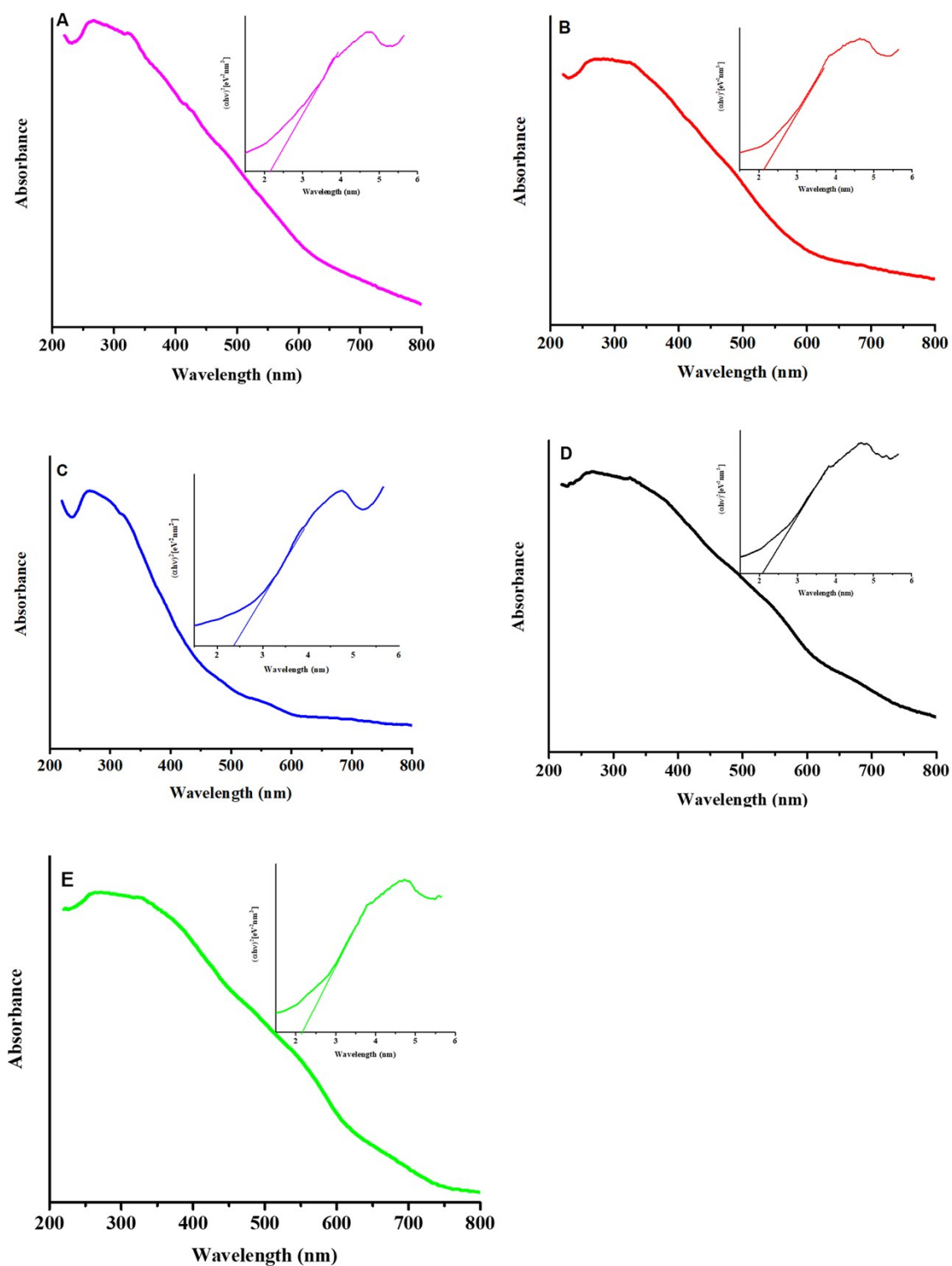


**Fig. S7.** Diffuse reflectance UV-vis spectra of STA-12-Fe-Mn, (A) 20:80, (B) 30:70, (C) 50:50, (D) 70:30, and (E) 80:20 (the insets are the tauc's plots).

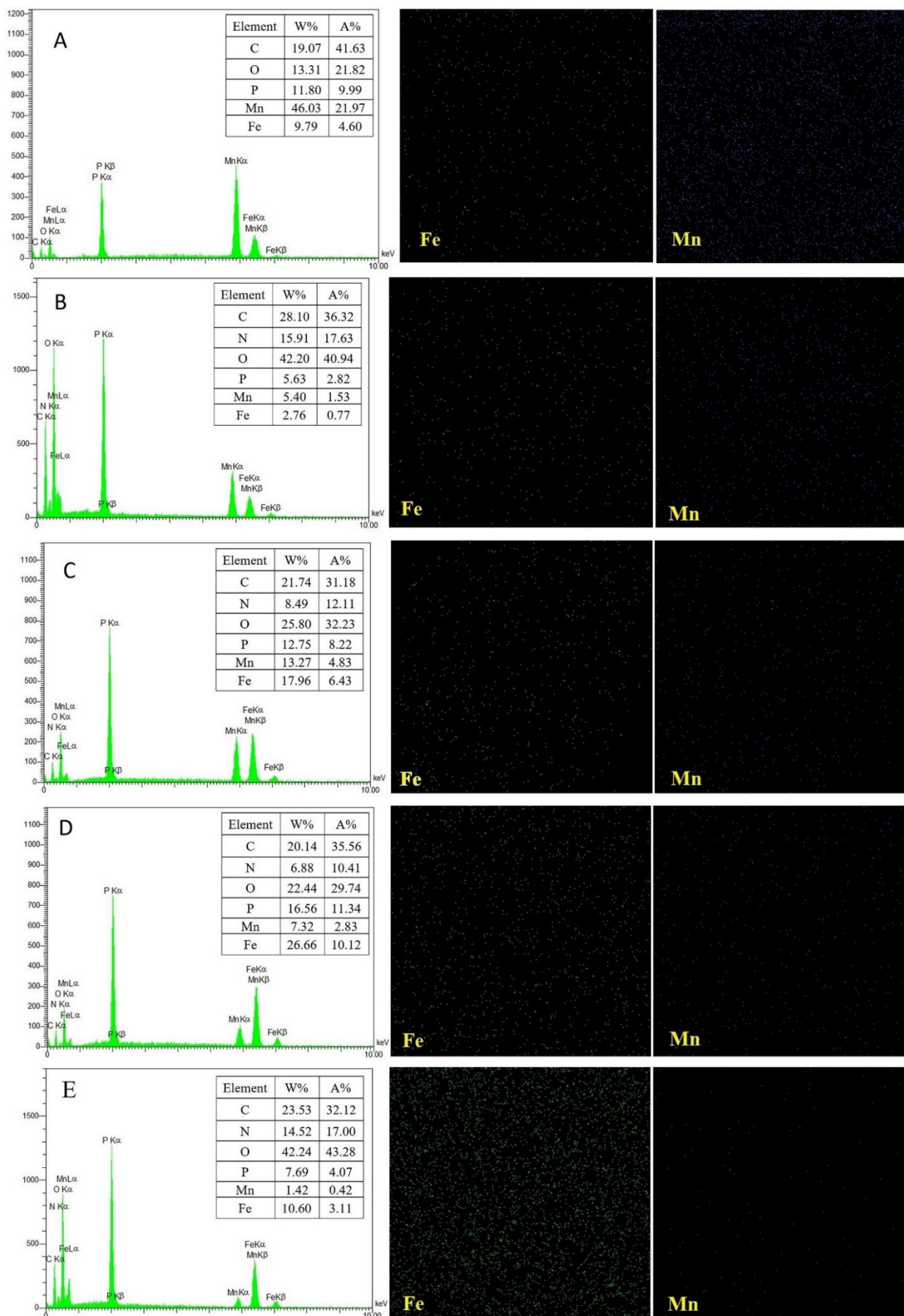


**Fig. S8.** EDS spectra and mappings of Mn/Fe content for as-prepared MOFs. STA-12-Mn-Fe (80:20) (A), (70:30) (B), (50:50) (C), (30:70) (D) and (20:80) (E).

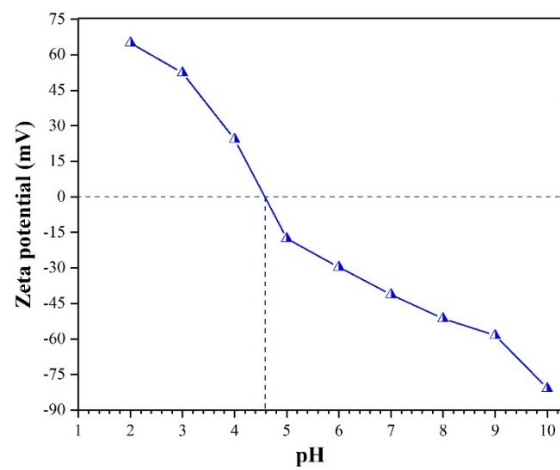


**Fig. S9.** Zeta-potential of STA-12-Mn-Fe (50:50) different pH.

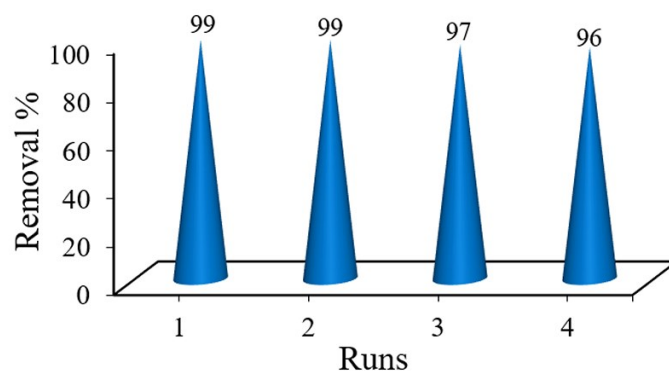


**Fig. S10.** Recyclability of STA-12-Mn-Fe (50:50)

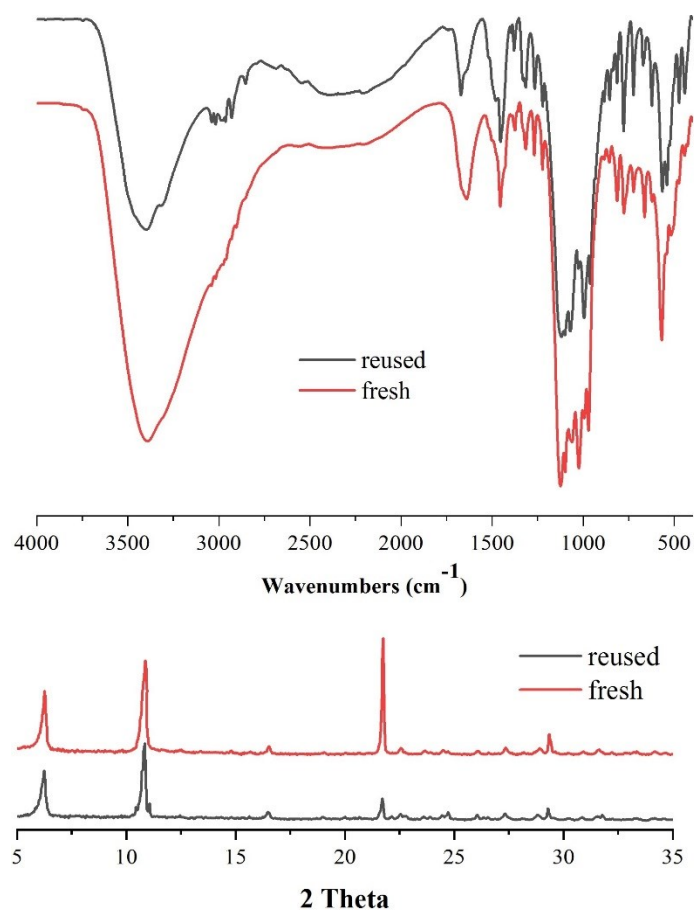


**Fig. S11.** FTIR spectra (up) and PXRD (down) of STA-12-Mn-Fe after four catalytic reactions.

**Table S2.** The ANOVA results of the response surface quadratic model for reduction of Cr(VI).

Source	Sum of Squares	df	Mean Square	F Value	p-value	
Block	684.92	2	342.46			
<b>Model</b>	20141.16	8	2517.65	87.22	< 0.0001	<b>significant</b>
A-pH	11617.32	1	11617.32	402.49	< 0.0001	
B-CrConc.	4115.23	1	4115.23	142.57	< 0.0001	
C-Cat	13.76	1	13.76	0.48	0.4983	
D-Time	85.69	1	85.69	2.97	0.1011	
AB	1809.44	1	1809.44	62.69	< 0.0001	
CD	610.71	1	610.71	21.16	0.0002	
A <sup>2</sup>	848.44	1	848.44	29.39	< 0.0001	
B <sup>2</sup>	1245.71	1	1245.71	43.16	< 0.0001	
Residual	548.41	19	28.86			
Lack of Fit	520.75	16	32.55	3.53	0.1633	<b>not significant</b>
Pure Error	27.67	3	9.22			
Cor Total	21374.49	29				

**Reference:**



[1] J. A. Groves, S. R. Miller, S. J. Warrender, C. Mellot-Draznieks, P. Lightfoot, P. A. Wright, *Chem. Commun.* **2006**, 3305.